JACS
JOURNAL OF THE AMERICAN CHEMICAL SOCIETY
Article
pubs.acs.org/JACS

Study of the Thermoelectric Properties of Lead Selenide Doped with Boron, Gallium, Indium, or Thallium

Qian Zhang,[†] Feng Cao,[†] Kevin Lukas,[†] Weishu Liu,[†] Keivan Esfarjani,[‡] Cyril Opeil,[†] David Broido,[†] David Parker,[§] David J. Singh,[§] Gang Chen,*[,‡] and Zhifeng Ren*[,†]

[†]Department of Physics, Boston College, Chestnut Hill, Massachusetts 02467, United States
[‡]Department of Mechanical Engineering, Massachusetts Institute of Technology, Cambridge, Massachusetts 02139, United States
[§]Materials Science and Technology Division, Oak Ridge National Laboratory, Oak Ridge, Tennessee 37831-6056, United States

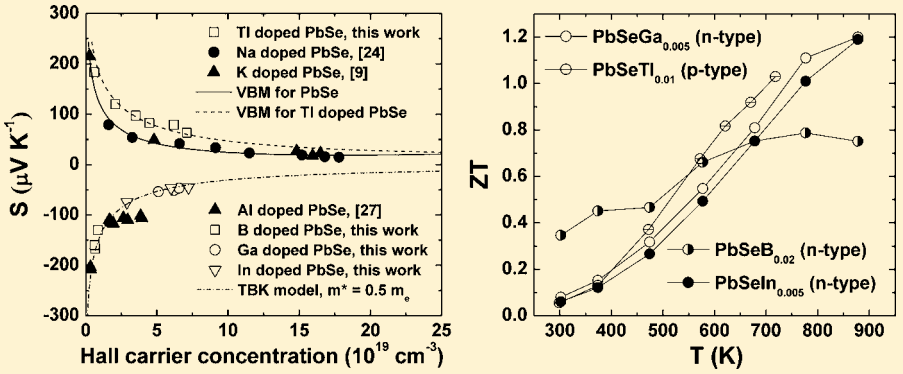

ABSTRACT: Group IIIA elements (B, Ga, In, and Tl) have been doped into PbSe for enhancement of thermoelectric properties. The electrical conductivity, Seebeck coefficient, and thermal conductivity were systematically studied. Room-temperature Hall measurements showed an effective increase in the electron concentration upon both Ga and In doping and the hole concentration upon Tl doping to ~7×10^{19} cm^{-3}. No resonant doping phenomenon was observed when PbSe was doped with B, Ga, or In. The highest room-temperature power factor ~2.5×10^{-3} W m^{-1} K^{-2} was obtained for PbSe doped with 2 atom % B. However, the power factor in B-doped samples decreased with increasing temperature, opposite to the trend for the other dopants. A figure of merit (ZT) of ~1.2 at ~873 K was achieved in PbSe doped with 0.5 atom % Ga or In. With Tl doping, modification of the band structure around the Fermi level helped to increase the Seebeck coefficient, and the lattice thermal conductivity decreased, probably as a result of effective phonon scattering by both the heavy Tl^{3+} ions and the increased grain boundary density after ball milling. The highest p-type ZT value was ~1.0 at ~723 K.

INTRODUCTION

Thermoelectric (TE) materials need high ZT values to be useful for applications. Here $ZT = [S^2\sigma/(\kappa_L+\kappa_e)]T$, and S is the Seebeck coefficient, σ the electrical conductivity, κ_L the lattice thermal conductivity, κ_e the electronic thermal conductivity, and T the absolute temperature.[1−3] With good ZT values found in both n- and p-type PbTe recently, PbTe is viewed as one of the best TE materials at mid-temperature range (400−800 K).[4−10] Most of the possible dopants have been studied for enhancement of ZT in PbTe by calculations or experiments.[11−17] Group IIIA elements have been found to be effective for controlling both the carrier concentration and the carrier type in this material.[11,18−22] It was found that group IIIA elements can be either acceptors[11,21] or donors.[18,19,22] Different models have been proposed to explain this amphoteric behavior.[20] Interestingly, In and Tl doping has been reported to induce resonant states in n- and p-type PbTe, respectively, which helps increase the Seebeck coefficient without correspondingly diminishing the electrical conductivity, therefore enhancing the ZT value.[11,19,21]

Another IV−VI narrow band gap semiconductor, PbSe, has drawn much attention because of several advantages.[23−27] Most of all, it also has decent doping optimized ZT.[24,27] Parker and Singh predict ZT as high as 2 at 1000 K if heavily doped with holes. A band flattening ~0.35−0.4 eV below the valence band edge helps the enhancement of the Seebeck coefficient,[23] and the increased band gap postpones the saturation of the Seebeck coefficient with increasing temperature. Na, K, and Ag are subsequently confirmed as good dopants offering high hole concentration and high $ZT > 1$.[9,24,28] For n-type PbSe, the conventional electron impurity Cl and I that work well in PbTe can also work in PbSe.[8,26,29] Additionally, the impact of Bi,[30] rare-earth elements (Ce, Pr, Nd, Eu, Gd, and Yb),[31] Pb and Se defects,[32] codopants of Na and Cd, and Mn have all been studied.[29] However, it is still interesting and perhaps controversial to consider group IIIA elements in PbSe.[25,27,33−36] Encouragingly, Al was found as an effective n-

Received: August 8, 2012
Published: October 1, 2012

   dx.doi.org/10.1021/ja307910u | J. Am. Chem. Soc. 2012, 134, 17731−17738

Table 1. Theoretical Density D_T, Measured Volumetric Density D, and Relative Density D_R for $PbSeB_x$, $PbSeGa_x$, $PbSeIn_x$, and $PbSeTl_x$

	$PbSeB_x$			$PbSeGa_x$			$PbSeIn_x$			$PbSeTl_x$		
comp.	0.01	0.02	0.03	0.003	0.005	0.007	0.003	0.005	0.007	0.005	0.010	0.020
D_T (g cm^{-3})	8.19	8.14	8.08	8.24	8.23	8.22	8.24	8.24	8.23	8.25	8.25	8.24
D (g cm^{-3})	7.85	7.87	7.87	7.98	7.94	8.00	8.00	7.9	7.92	7.73	7.68	7.56
D_R	96%	97%	97%	97%	96%	97%	97%	96%	96%	94%	93%	92%

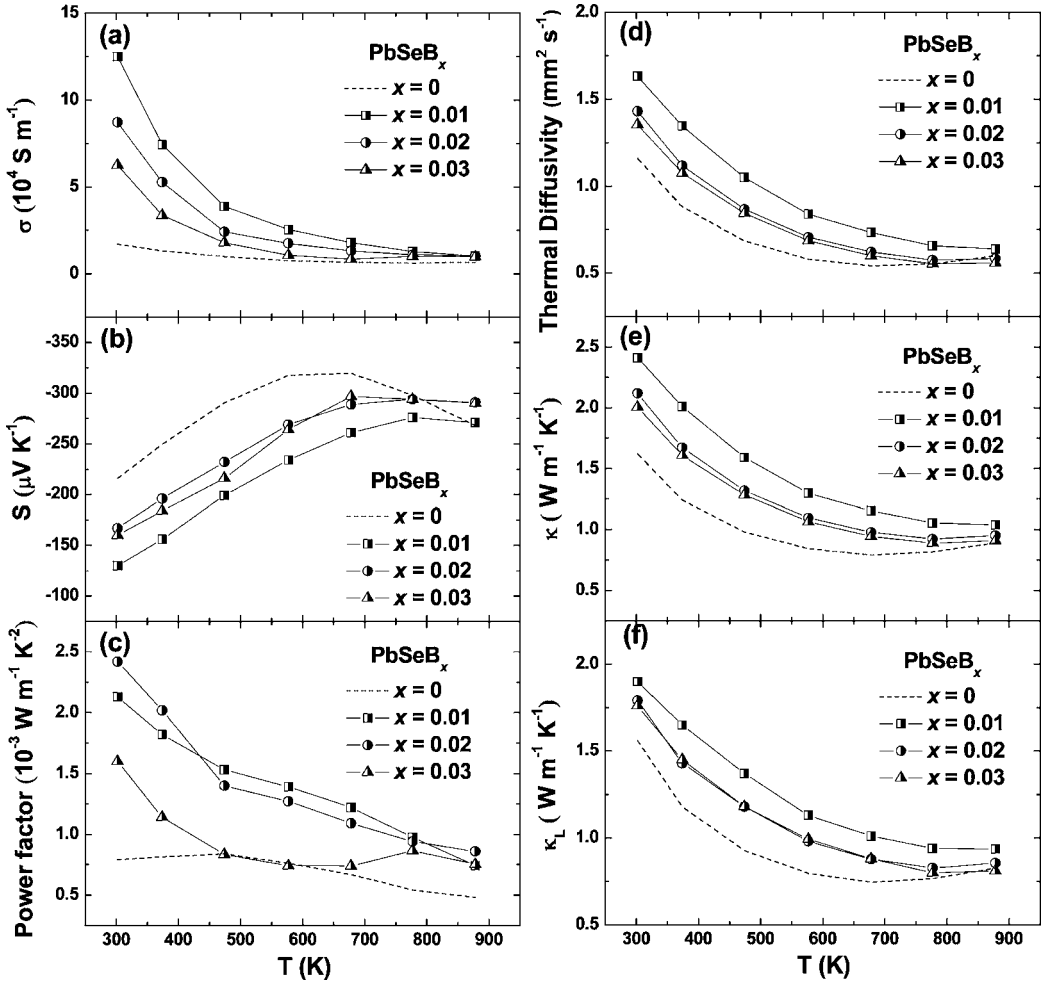

Figure 1. Temperature dependence of (a) electrical conductivity, (b) Seebeck coefficient, (c) power factor, (d) thermal diffusivity, (e) total thermal conductivity, and (f) lattice thermal conductivity for $PbSeB_x$ (x = 0, 0.01, 0.02, and 0.03).

type dopant in PbSe, which can create resonant states for the enhancement of ZT,[27] like Tl in p-type PbTe.[11,21,37,38] It was also suggested that In and Tl create resonant levels in PbSe without strong experimental evidence.[33−35] Recent results by the first-principles calculations concluded that the resonant states in Tl- and In-doped PbSe extend largely into the band gap and even the conduction band, respectively, which degrades the TE properties.[36] In this paper, we report systematic experimental study on the doping effect of group IIIA elements (B, Ga, In, and Tl) on thermoelectric properties of PbSe. The electrical conductivity, Seebeck coefficient, and thermal conductivity of samples with different doping concentrations are investigated. The comparison of all group IIIA elements doping in PbSe is presented. In spite of the absence of resonant states, ZT of ∼1.2 is obtained in both 0.5 at % Ga-doped n-type PbSe and 0.5 at % In-doped n-type PbSe at ∼873 K. The band structure modification around Fermi level and reduced lattice thermal conductivity help the ZT reach ∼1.0 at about 723 K for Tl-doped p-type PbSe.

EXPERIMENTAL SECTION

Synthesis. Samples with nominal compositions $PbSeB_x$ (boron powder 99.99%, x = 0.01, 0.02, and 0.03), $PbSeGa_x$ (gallium ingots 99.99%, x = 0.003, 0.005, and 0.007), $PbSeIn_x$ (indium powder 99.99%, x = 0.003, 0.005, and 0.007), and $PbSeTl_x$ (thallium granules 99.99%, x = 0.00125, 0.0025, 0.005, 0.01, 0.015, and 0.02) were prepared by melting the materials inside a quartz tube with carbon coating. The detailed procedure can be found in our previous report.[9] The same compositions of $PbSeTl_x$ (x = 0, 0.00125, 0.0025, 0.005, 0.01, 0.015, and 0.02) were also prepared by mechanical alloying due to the difficulty of doping Tl into the PbSe lattice by a melting method. In the case of ball milling, the raw materials Tl (granules, 99.99%), Pb (granules, 99.99%), and Se (granules, 99.99%) were sealed directly in the stainless steel jar inside an argon-filled glovebox and ball milled by a high-energy ball mill SPEX 8000D (SPEX Sample

dx.doi.org/10.1021/ja307910u | J. Am. Chem. Soc. 2012, 134, 17731−17738

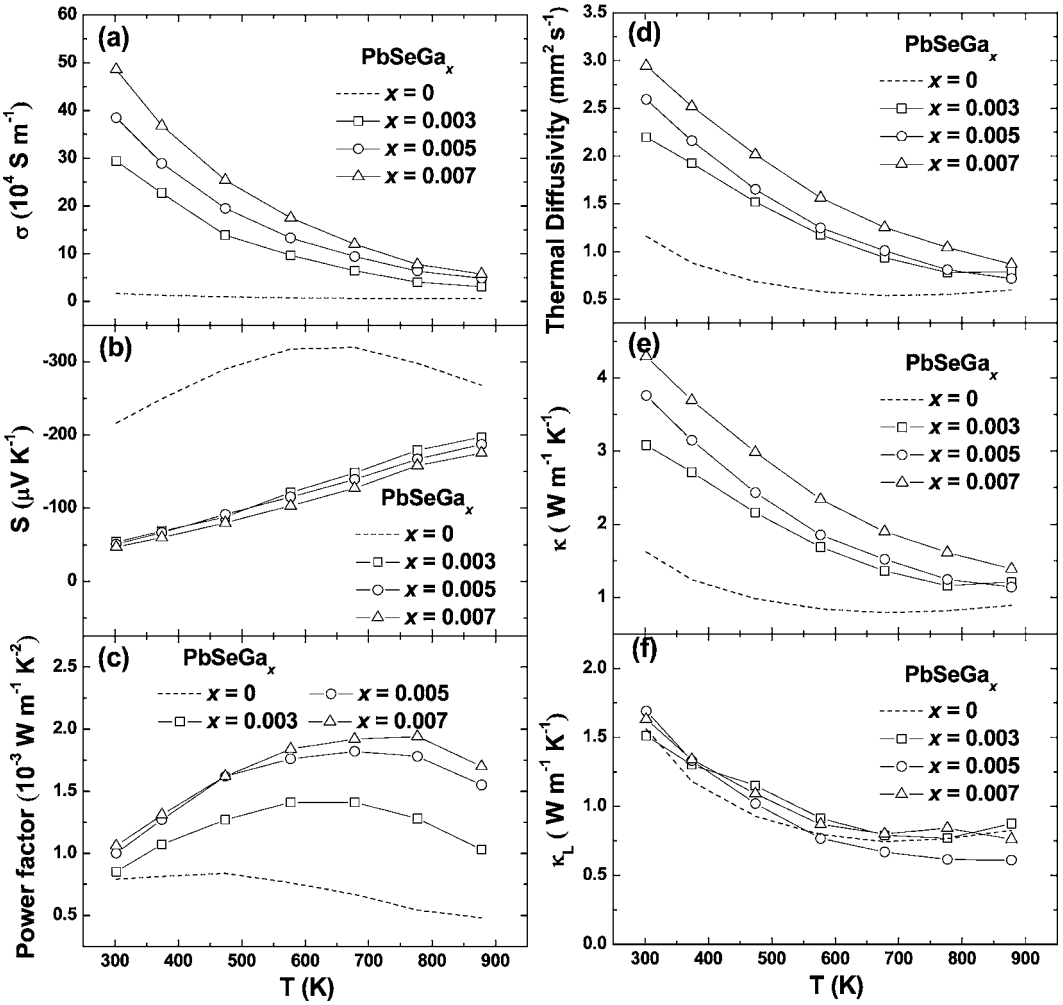

Figure 2. Temperature dependence of (a) electrical conductivity, (b) Seebeck coefficient, (c) power factor, (d) thermal diffusivity, (e) total thermal conductivity, and (f) lattice thermal conductivity for $PbSeGa_x$ (x = 0, 0.003, 0.005, and 0.007).

Prep.). The obtained powder was loaded into the graphite die and consolidated by direct current (dc)-induced hot pressing.

Characterizations. X-ray diffraction spectra analysis was conducted on a PANalytical multipurpose diffractometer with an X'celerator detector (PANalytical X'Pert Pro). All samples are confirmed in a single phase. The microstructures were investigated by a scanning electron microscope (SEM, JEOL 6340F). The electrical resistivity (ρ) and Seebeck coefficient (S) were simultaneously measured on a commercial system (ULVAC ZEM-3). The thermal conductivity κ was calculated using $\kappa = D\alpha C_p$, where D is volumetric density determined by the Archimedes method and shown in Table 1 compared with the theoretical density D_T, α the thermal diffusivity obtained on a laser flash apparatus (Netzsch LFA 457), and C_p the specific heat measured on a differential scanning calorimetry thermal analyzer (Netzsch DSC 404 C). The Hall Coefficient R_H at room temperature was measured using the Physical Properties Measurement System (PPMS, Quantum Design). The Hall carrier concentration n_H and mobility μ_H were calculated using $n_H = 1/(eR_H)$ and $\mu_H = \sigma R_H$, respectively. The uncertainty for the electrical conductivity is 3%, the Seebeck coefficient 5%, and the thermal conductivity 4%, so the combined uncertainty for the power factor is 10% and that for the ZT value is 11%.[39] Error bars were not used in the figures to increase the readability of the curves.

RESULTS AND DISCUSSION

Different compositions are prepared for optimization of the TE properties. Figures 1, 2, and 3 present the (a) electrical conductivity, (b) Seebeck coefficient, (c) power factor, (d) thermal diffusivity, (e) total thermal conductivity, and (f) lattice thermal conductivity of three samples for each kind of doping, $PbSeB_x$ (x = 0, 0.01, 0.02, and 0.03), $PbSeGa_x$ (x = 0, 0.003, 0.005, and 0.007), and $PbSeIn_x$ (x = 0, 0.003, 0.005, and 0.007), respectively. The properties of undoped PbSe were reported in the previous work.[9] All compositions are nominal, but the real composition is very close to the nominal since there was no noticeable mass loss during the sample preparation process. All doping can increase the electrical conductivity. With increasing temperature, the electrical conductivity decreases, and the Seebeck coefficient increases. The Seebeck coefficient increases without a sign of bipolar effect with Ga or In doping. However, the Seebeck coefficient saturates at ~400−500 °C in B-doped PbSe with lower carrier concentration. All three dopings are n-type with a negative Seebeck coefficient. The highest power factor is ~2.5 × 10^{-3} W m^{-1} K^{-2} at room temperature for the 2 at % B-doped PbSe, ~2.0 × 10^{-3} W m^{-1} K^{-2} at 500 °C for 0.7 at % Ga-doped PbSe. In a conservative way, the C_p of $PbSeB_{0.03}$, $PbSeGa_{0.007}$, $PbSeIn_{0.007}$, and $PbSeTl_{0.02}$ is used for the calculation of the total thermal conductivity of each kind of doping, shown in Figure 4. All the total thermal conductivities decrease with increasing temperature. By subtracting the electronic thermal conductivity from the total thermal conductivity ($\kappa_L = \kappa_{total} - \kappa_e = \kappa_{total} - L\sigma T$, where L is the

dx.doi.org/10.1021/ja307910u | J. Am. Chem. Soc. 2012, 134, 17731−17738

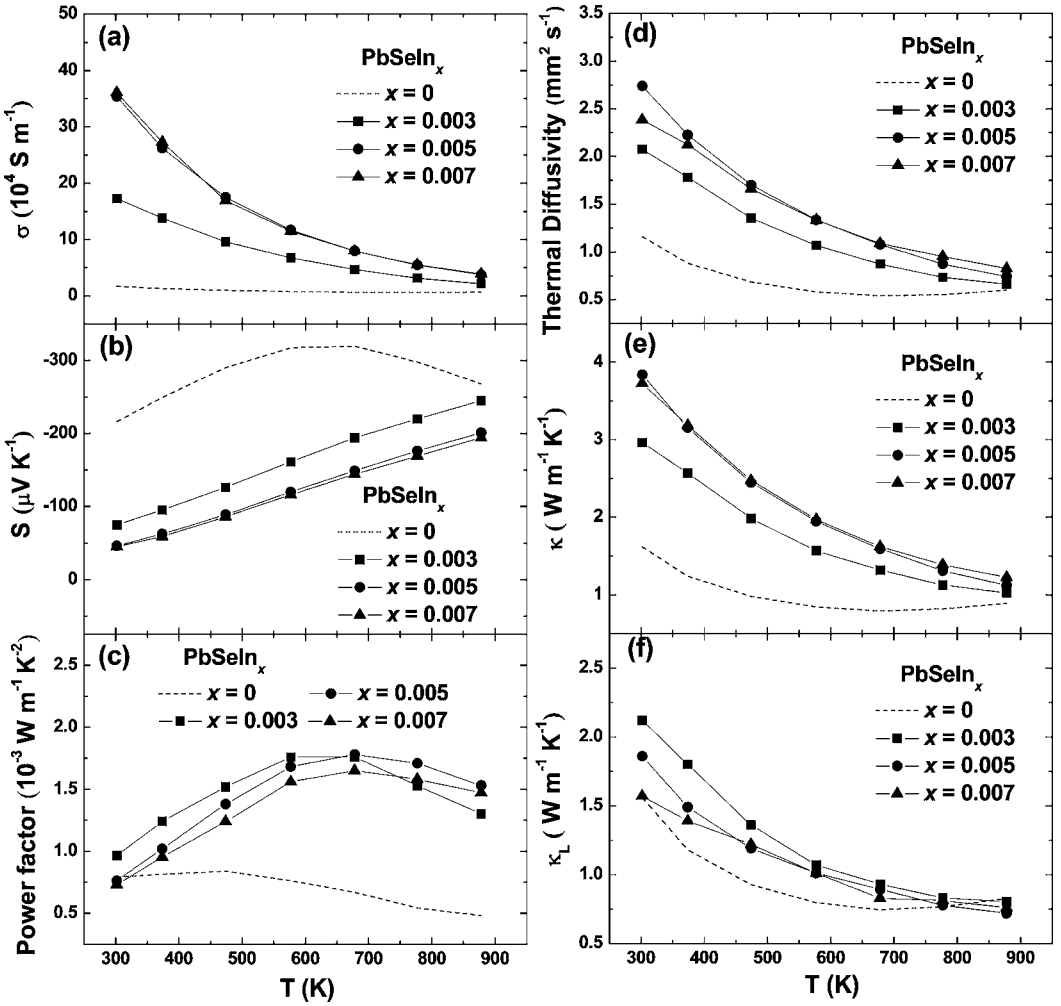

Figure 3. Temperature dependence of (a) electrical conductivity, (b) Seebeck coefficient, (c) power factor, (d) thermal diffusivity, (e) total thermal conductivity, and (f) lattice thermal conductivity for $PbSeIn_x$ (x = 0, 0.003, 0.005, and 0.007).

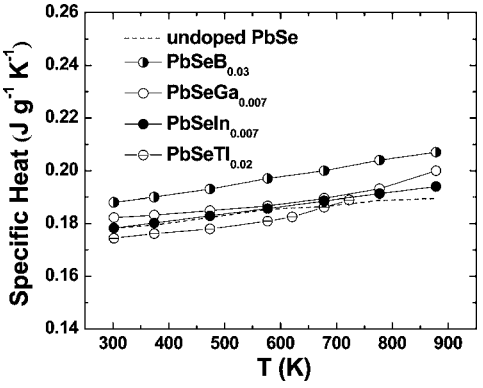

Figure 4. Temperature dependence of specific heat for $PbSeB_{0.03}$, $PbSeGa_{0.007}$, $PbSeIn_{0.007}$, $PbSeTl_{0.02}$, and undoped PbSe.

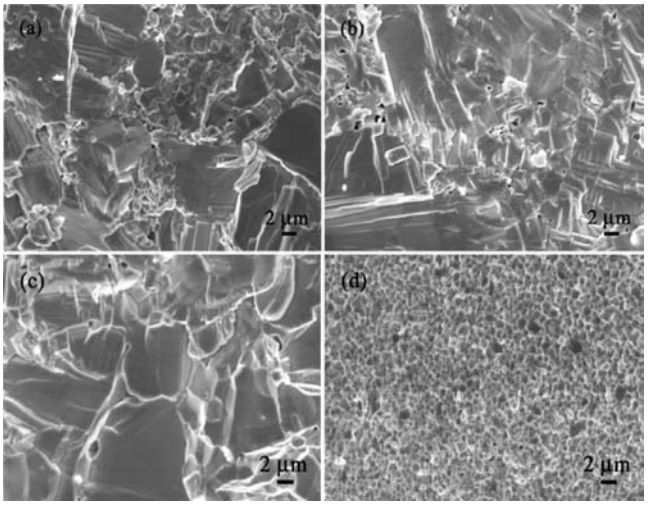

Figure 5. Representative SEM images of hot pressed (a) $PbSeB_{0.02}$, (b) $PbSeGa_{0.005}$, (c) $PbSeIn_{0.005}$, and (d) $PbSeTl_{0.01}$.

Lorenz number calculated using a two-band model),[9,40] the lattice thermal conductivity is obtained. In spite of the lowest total thermal conductivity, B-doped PbSe has the highest lattice thermal conductivity because of the weakest phonon scattering by the lightest B^{3+} compared with Ga^{3+} and In^{3+}. In addition, we present the fresh cross-section microstructures of the samples with different dopings in Figure 5a–d (Figure 5d will be discussed later). It shows relatively large grain sizes ~10 μm made by hand milling. Compared with ball-milled Al-doped PbSe,[27] the overall lattice thermal conductivity is higher, which further confirms the beneficial effect of ball milling.

Together with Al-doped PbSe (filled triangles),[27] we plot a room-temperature Seebeck coefficient as a function of Hall carrier concentration for B- (half open circles), Ga- (open

dx.doi.org/10.1021/ja307910u | J. Am. Chem. Soc. 2012, 134, 17731–17738

circles), and In-doped PbSe (solid circles) in Figure 6 to clearly show the band information. With the decreasing difference in

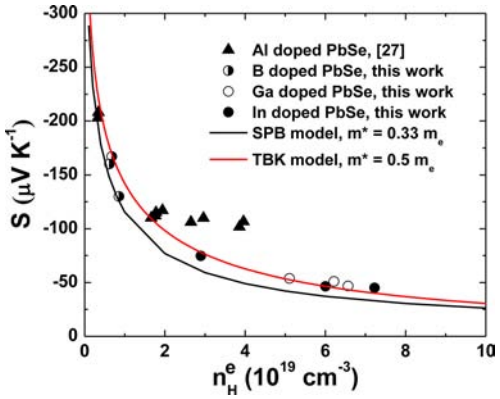

Figure 6. Room-temperature Pisarenko plots for $PbSeB_x$ (x = 0.01, 0.02, and 0.03, half open circles), $PbSeGa_x$ (x = 0.003, 0.005, and 0.007, open circles), and $PbSeIn_x$ (x = 0.003, 0.005, and 0.007, solid circles) in comparison with reported data on Al-doped PbSe by Zhang et al.[27] (solid triangles). Black curve is based on SPB model with the electron effective mass of PbSe m^*/m_e = 0.33. Red curve is based on nonparabolic TBK model with the electron effective mass of PbSe m^*/m_e = 0.5.

ionic radius between dopants and Pb, the optimized carrier concentration increases. It is difficult to further increase the carrier concentration of B-doped PbSe because of the small ionic radius of B. High carrier concentration $\sim 7 \times 10^{19}$ cm^{-3} is obtained in both Ga- and In-doped PbSe. The Seebeck coefficients of all the samples decrease with increasing carrier concentration. The measured Seebeck coefficient values are compared with calculated results from two models: In both models, the deformation potential scattering by acoustic phonons was taken to be the dominant carrier scattering mechanism consistent with previous work.[4,13,40] In the first model, a single parabolic band (SPB) is used with effective mass m^*/m_e = 0.33 (black curve). Note that this curve deviates slightly from the data in spite of consideration of the Hall factor.[7,25] In the second model, the nonparabolicity of conduction band of PbSe is included using a two-band Kane (TBK) model,[8,40] which describes the conduction and light hole valence bands about the L-point. The TBK model fits the data well using a much larger effective mass m^*/m_e = 0.5 (red curve), which is close to the optical measurement results.[25] It is clear that no matter which model we use, Al-doped PbSe does not fit the curve. This could be due to resonant scattering.[27]

There are neither resonant states to explain the high Seebeck coefficient nor strong phonon scattering to produce low lattice thermal conductivity demonstrated in these materials. However, the highest ZT values (Figure 7) reach ~1.2 in 0.5 at % Ga- or In-doped PbSe at about 873 K, which is attributed to the high-concentration doping. In Table 2, comparison of room-temperature electrical properties of the optimally doped PbSe using different dopants is presented. Lower carrier concentration and reduced Hall mobility by resonant doping restrict further improvement of Al-doped PbSe. We tried to codope PbSe with Al and Ga or Al and In, but this strategy did not lead to a ZT enhancement. With a low power factor and high lattice thermal conductivity at high temperature, the highest ZT value for B-doped PbSe is only ~0.8 at about 773 K. This ZT value is still comparable with Ga- and In-doped PbSe measured directly

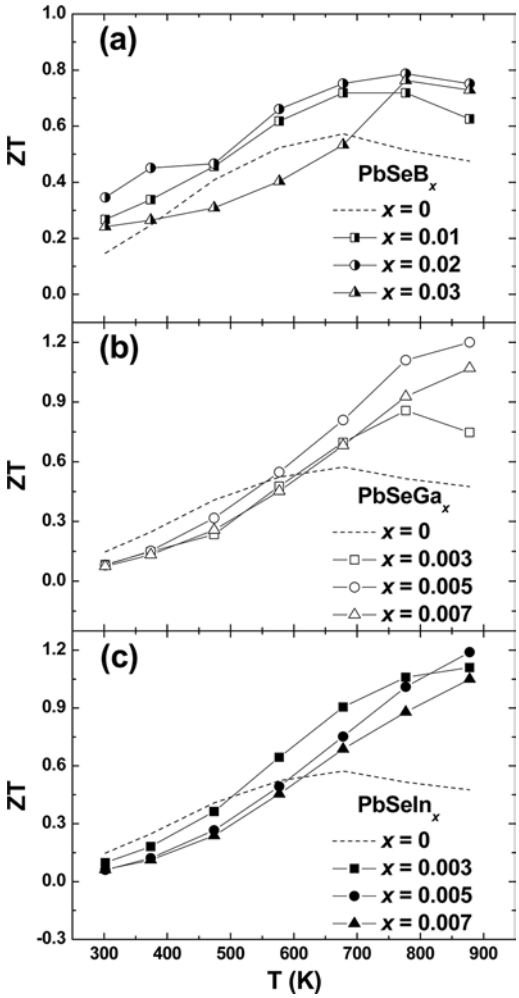

Figure 7. Temperature dependence of ZT for (a) $PbSeB_x$ (x = 0, 0.01, 0.02, and 0.03), (b) $PbSeGa_x$ (x = 0, 0.003, 0.005, and 0.007), and (c) $PbSeIn_x$ (x = 0, 0.003, 0.005, and 0.007).

from the ingot specimens by melting.[25] Despite the lower peak ZT of B-doped PbSe, the temperature-averaged ZT is comparable with the Ga- and In-doped PbSe obtained in this work.

It is also worth noting that at all but the highest temperatures measured, the lattice thermal conductivity is the predominant component of the thermal conductivity. For example, in Figure 1 (boron doping) the lattice component at 500 K is approximately 1.2 W m^{-1} K^{-1}, while the electronic portion is roughly 0.3 W m^{-1} K^{-1}. The figure of merit ZT can be rewritten as

$$ZT = S^2\sigma T/\kappa = S^2 r/L \quad (1)$$

with S the thermopower, σ the electrical conductivity, κ the thermal conductivity, r the ratio of electronic and total (i.e., lattice + electronic) thermal conductivity, and L the Lorenz number, in the Wiedemann–Franz relation, nominally L = 2.45 × 10^{-8} V^2 K^{-2}. With r in this case at 0.2 combined with the Seebeck coefficient of approximately −225 μV K^{-1}, one finds, as in the experiment, a relatively low ZT of ~0.4 at 500 K. However, if it were possible to reduce the lattice thermal conductivity without comparably affecting the charge carrier mobility, the ratio r would increase and substantial increases in ZT at this temperature, and in fact in the whole temperature

dx.doi.org/10.1021/ja307910u | J. Am. Chem. Soc. 2012, 134, 17731−17738

Table 2. Comparison of Room-Temperature Electrical Properties for Optimally Doped PbSe by B or Al,[27] Ga, In, and Tl

	B	Al	Ga	In	Tl
composition	$PbSeB_{0.02}$	$PbSeAl_{0.01}$	$PbSeGa_{0.005}$	$PbSeIn_{0.005}$	$PbSeTl_{0.01}$
σ (10^4 S m^{-1})	8.72	12.9	38.5	35.4	3.97
S (μV K^{-1})	−167	−117	−51	−46.4	82.8
n_H (10^{19} cm^{-3})	0.677	1.94	6.215	6	4.475
μ_H (cm^2 V^{-1} s^{-1})	827	416	465	433	39

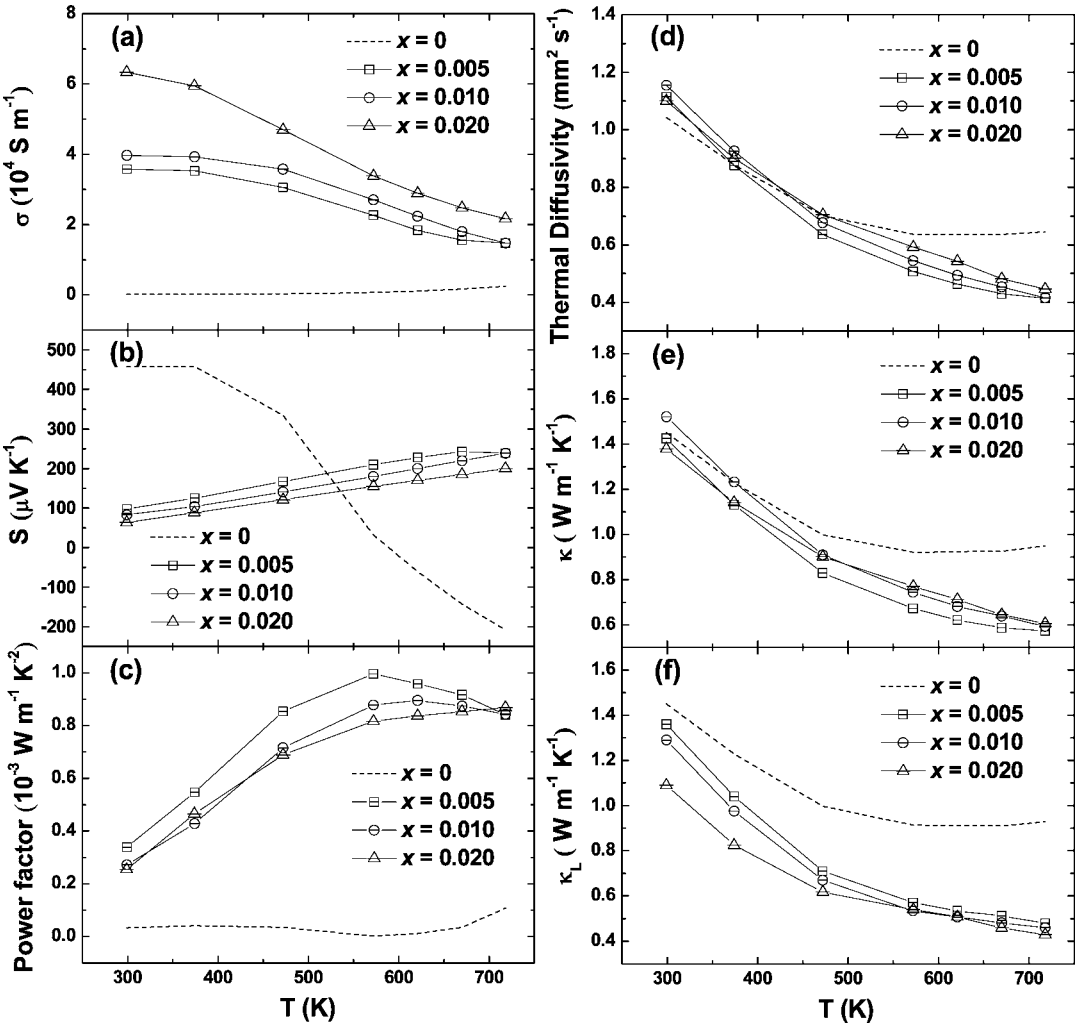

Figure 8. Temperature dependence of (a) electrical conductivity, (b) Seebeck coefficient, (c) power factor, (d) thermal diffusivity, (e) total thermal conductivity, and (f) lattice thermal conductivity for $PbSeTl_x$ (x = 0, 0.005, 0.01, and 0.02).

range from 300 to 700 K would be possible. Such a lattice thermal conductivity reduction has already been shown possible in ref 41, where a ZT of 1.4 for Bi_2Te_3 was found, significantly higher than the "optimized" value of 1.0 in bulk, which itself includes alloying optimization, which was not performed here and could itself have a beneficial impact if applied here.

Such an optimization would generally require, in the lowest temperature range from 300 to 500 K, lower doping levels than the best values here, with optimal doping ranges increasing with temperature. Reducing the temperature where ZT is maximum in PbSe is of interest for solar thermal and waste heat recovery applications.

Like Tl doping in PbTe,[11] Tl in PbSe also acts as acceptor, different from other group IIIA elements. The electrical conductivity, Seebeck coefficient, power factor, thermal diffusivity, total thermal conductivity, and lattice thermal conductivity for $PbSeTl_x$ (x = 0, 0.005, 0.01, and 0.02) are shown in Figure 8. It should be noted that all the properties presented for Tl-doped samples are on material that was prepared by ball milling directly. We also tried Tl-doped PbSe by melting and hand milling, as we did for B-, Ga-, and In-doped PbSe, but the properties are quite poor because Tl could not be doped into the lattice during melting process. This situation is similar for Al-doped PbSe and requires further studies. With increasing content of Tl, the electrical conductivity increases, but the Seebeck coefficient and the power factor decrease. The maximum power factor is only ~1.0 × 10^{-3} W m^{-1} K^{-2} at 300 °C for 0.5 at % Tl-doped PbSe, much lower than that of B- or Al-,[27] Ga-, and In-doped PbSe. However, the lattice thermal conductivity is as low as ~0.43 W

dx.doi.org/10.1021/ja307910u | J. Am. Chem. Soc. 2012, 134, 17731−17738

m^{-1} K^{-1} at about 720 K, lower than other dopings in all the measured temperature range. It is the result of stronger phonon scattering by heavier Tl^{3+} ion as well as the increased mid-to-long wavelength phonon scattering by increased boundary scattering, corresponding to the grain structure shown in Figure 5d. The grain size is only ~200−500 nm, even smaller than ball-milled Al-doped PbSe.[27] However it is puzzling why the thermal conductivity of the pure PbSe is so much higher for a similar grain size. We did not further study this due to the very low ZT for the pure PbSe.

The room-temperature Pisarenko plot for Tl-doped PbSe (open circles) is shown in Figure 9 to elucidate the electrical transport. For comparison, we also presented other reported p-type PbSe doped with Na (open squares)[24] and K (open triangles)[9] and also p-type PbTe doped with Tl (solid circles),[11] Na (solid squares),[16] and K (solid triangles).[9] Similar to PbTe, PbSe has a light hole region at the valence band maximum and a heavier band behavior ~0.35−0.4 eV below this.[13] To fit the data, the two-band Kane model described before is combined with an additional parabolic heavy hole portion of the valence band. We refer this as the valence band model (VBM). Again, scattering of holes is assumed to be by acoustic phonons through the deformation potential interaction. Further details of the VBM can be found elsewhere.[9] Due to the contribution from the heavy hole portion in PbTe, the Seebeck coefficient remains unchanged when heavily doped. Especially when Tl is doped, the Seebeck coefficient is as high as ~130 μV K^{-1}.[11] This Tl-doped PbTe is an excellent thermoelectric material. PbSe has qualitatively similar valence band features, in particular light holes at the valence band edge and a crossover to heavier behavior at high doping levels.[9,13,24] However, the heavy hole region only contributes at high temperatures, with almost the same trend like having one band at room temperature. The Seebeck coefficient decreases all the way with increasing carrier concentration in Na- and K-doped PbSe and falls well on the line calculated using the VBM, which is also not much different from the TBK model at room temperature.[9] Interestingly, we found the same trend happens in Tl-doped PbSe with increased Seebeck coefficient ~50 μV K^{-1} for each corresponding carrier concentration, which can be fitted by VBM using light hole effective mass m^*_{lh}/m_e = 0.7 (dashed black line), much higher than for Na-doped PbSe m^*_{lh}/m_e = 0.4 (solid black line). In previous *ab initio* calculations, it was found that there is local increase of DOS in Tl-doped PbSe, however, the impurity states reside in the band gap, which degrades the increase of Seebeck coefficient and makes it even lower than Na-doped PbSe.[36] Our data shown in Figure 9 have a small abnormality at $n_H^P = 6 \times 10^{19}$ cm^{-3} in qualitative agreement with the first-principles calculations of ref 36, Figure 12b. It shows an increase in the Seebeck coefficient, which is possibly due to some band modifications by Tl doping near Fermi level. In Table 1, the low Hall mobility of Tl-doped PbSe may be the result of increased scattering by modulated effective mass, which lowers the electrical conductivity as well as power factor.

The highest ZT value of Tl-doped PbSe is ~1.0 at about 723 K, shown in Figure 10. It is lower than that of Tl-doped PbTe.[17] With increasing temperature, the ZT value increases, showing no sign of decreasing for 1 at % and 2 at % Tl-doped PbSe. However, the highest mechanically stable temperature for all the ball-milled Tl-doped samples is ~750 K, which is consistent with ball-milled Tl-doped PbTe.[10,21] It seems that with increasing ionic radius of dopants, the stable temperature decreases for ball-milled IIIA-doped PbSe samples. As in the case of PbTe, it is also possible to include silicon and sodium together in Tl-doped PbSe. It may be possible to use this to produce stable samples at higher temperature and enhance ZT.[10]

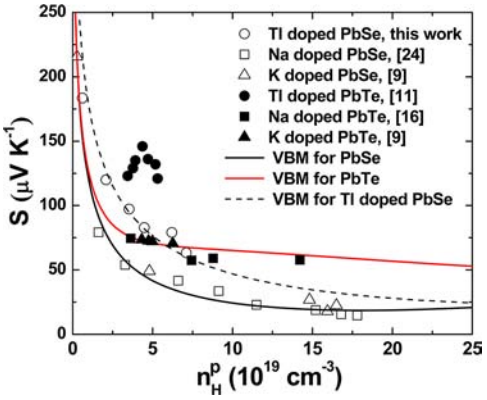

Figure 9. Room-temperature Pisarenko plots for $PbSeTl_x$ (x = 0.00125, 0.0025, 0.005, 0.01, 0.015, and 0.02, open circles) in comparison with the reported data on K-doped PbTe (solid triangles),[9] K-doped PbSe (open triangles),[5] Na-doped PbTe by Pei et al.[16] (solid squares), Na-doped PbSe by Wang et al.[24] (open squares), and Tl-doped PbTe by Heremans et al.[11] (solid circles). The solid black curve is based on a VBM for PbSe, and the solid red curve is based on a VBM for PbTe.[9] The dashed black curve is based on a VBM for Tl-doped PbSe. For PbTe, we use heavy hole effective mass m^*_{hh}/m_e = 2 and a separation between light hole portion and heavy hole portion of 0.12 eV. For PbSe, we use heavy hole effective mass m^*_{hh}/m_e = 2.5 and a separation between light and heavy hole portions of 0.26 eV. The light hole effective mass m^*_{lh}/m_e = 0.4 for Na-doped PbSe and m^*_{lh}/m_e = 0.7 for Tl-doped PbSe.

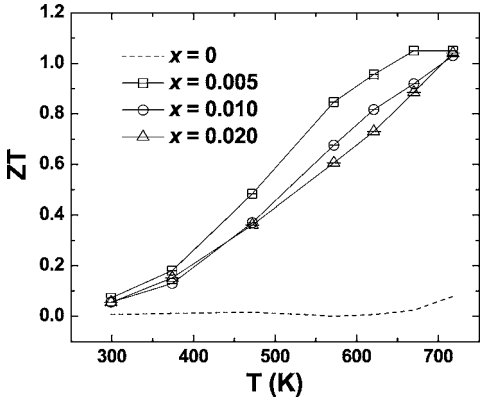

Figure 10. Temperature dependence of ZT for $PbSeTl_x$ (x = 0, 0.005, 0.01, and 0.02).

CONCLUSIONS

The detailed effect of B or Ga, In, and Tl doping on the thermoelectric properties of PbSe has been studied. There is no evidence for resonant states in B-, Ga-, or In-doped PbSe, but it seems that there may be band structure modification by Tl doping around the Fermi level. Relatively high Seebeck coefficients are obtained in B-doped n-type PbSe, even though the maximum obtainable carrier concentration is limited, and Tl-doped p-type PbSe with high DOS effective mass but low

Hall carrier mobility. The highest ZT value obtained is ~1.2 in 0.5 at % Ga- or In-doped n-type PbSe at about 873 K. Due to the large reduction in lattice thermal conductivity by ball milling, Tl-doped PbSe has a maximum ZT of ~1.0 at about 723 K.

AUTHOR INFORMATION

Corresponding Author

gchen2@mit.edu; renzh@bc.edu

Notes

The authors declare no competing financial interest.

ACKNOWLEDGMENTS

This work is supported by "Solid State Solar Thermal Energy Conversion Center (S^3TEC)", an Energy Frontier Research Center funded by the U.S. Department of Energy, Office of Science, Office of Basic Energy Science under award number DE-SC0001299 (D.B., G.C., C.O., D.P., D.J.S., and Z.F.R.).

REFERENCES

(1) Majumdar, A. *Science* **2004**, *303*, 777.
(2) Rowe, D. M. *CRC Handbook of Thermoelectrics, Macro to Nano*; CRC Press, Taylor & Francis Group: Boca Raton, FL, 2006.
(3) Kraemer, D.; Poudel, B.; Feng, H. P.; Cavlor, J. C.; Yu, B.; Yan, X.; Ma, Y.; Wang, X. W.; Wang, D. Z.; Muto, A.; McEnaney, K.; Chiesa, M.; Ren, Z. F.; Chen, G. *Nat. Mater.* **2011**, *10*, 532.
(4) Pei, Y. Z.; Shi, X. Y.; LaLonde, A.; Wang, H.; Chen, L. D.; Snyder, G. J. *Nature* **2011**, *473*, 66.
(5) Pei, Y. Z.; LaLonde, A. D.; Heinz, N. A.; Shi, X. Y.; Lwanaga, S.; Wang, H.; Chen, L. D.; Snyder, G. J. *Adv. Mater.* **2011**, *23*, 5674.
(6) Biswas, K.; He, J. Q.; Zhang, Q. C.; Wang, G. Y.; Uher, C.; Dravid, V. P.; Kanatzidis, M. G. *Nat. Chem.* **2011**, *3*, 160.
(7) Pei, Y. Z.; Lensch-Falk, J.; Toberer, E. S.; Medlin, D. L.; Snyder, G. J. *Adv. Funct. Mater.* **2011**, *21*, 241.
(8) LaLonde, A. D.; Pei, Y. Z.; Snyder, G. J. *Energy Environ. Sci.* **2011**, *4*, 2090.
(9) Zhang, Q.; Cao, F.; Liu, W. S.; Lukas, K.; Yu, B.; Chen, S.; Opeil, C.; Chen, G.; Ren, Z. F. *J. Am. Chem. Soc.* **2012**, *134*, 10031.
(10) Zhang, Q. Y.; Wang, H. Z.; Zhang, Q.; Liu, W. S.; Yu, B.; Wang, H.; Wang, D. Z.; Ni, G.; Chen, G.; Ren, Z. F. *Nano Lett.* **2012**, *12*, 2324.
(11) Heremans, J. P.; Jovovic, V.; Toberer, E. S.; Saramat, A.; Kurosaki, K.; Charoenphakdee, A.; Yamanaka, S.; Snyder, G. J. *Science* **2008**, *321*, 554.
(12) Zhang, Q.; Sun, T.; Cao, F.; Li, M.; Hong, M. H.; Yuan, J. K.; Yan, Q. Y.; Hng, H. H.; Wu, N. Q.; Liu, X. G. *Nanoscale* **2012**, *2*, 1256.
(13) Singh, D. J. *Phys. Rev. B* **2010**, *81*, 195217.
(14) König, J. D.; Nielsen, M. D.; Gao, Y. B.; Winkler, M.; Jacquot, A.; Böttner, H.; Heremans, J. P. *Phys. Rev. B* **2011**, *84*, 205126.
(15) Guch, M.; Sankar, C. R.; Salvador, J.; Meisner, G.; Klernke, H. *Sci. Adv. Mater.* **2011**, *3*, 615.
(16) Pei, Y. Z.; LaLonde, A.; Iwanaga, S.; Snyder, G. J. *Energy Environ. Sci.* **2011**, *4*, 2085.
(17) Nielsen, M. D.; Levin, E. M.; Jaworski, C. M.; Schmidt-Rohr, K.; Heremans, J. P. *Phys. Rev. B* **2012**, *85*, 045210.
(18) Volkov, B. A.; Ryabova, L. I.; Khokhlov, D. R. *Phys. Usp.* **2002**, *45*, 819.
(19) Jovovic, V.; Thiagarajan, S. J.; Heremans, J. P.; Komissarova, T.; Khokhlov, D.; Nicorici, A. *J. Appl. Phys.* **2008**, *103*, 053710.
(20) Xiong, K.; Lee, G.; Gupta, R. P.; Wang, W.; Gnade, B. E.; Cho, K. *J. Phys. D: Appl. Phys.* **2010**, *43*, 405403 (8pp).
(21) Yu, B.; Zhang, Q. Y.; Wang, H.; Wang, X. W.; Wang, H. Z.; Wang, D. Z.; Snyder, G. J.; Chen, G.; Ren, Z. F. *J. Appl. Phys.* **2010**, *108*, 016104.
(22) Jaworski, C. M.; Heremans, J. P. *Phys. Rev. B* **2012**, *85*, 033204.
(23) Parker, D.; Singh, D. J. *Phys. Rev. B* **2010**, *82*, 035204.
(24) Wang, H.; Pei, Y. Z.; LaLonde, A. D.; Snyder, G. J. *Adv. Mater.* **2011**, *23*, 1366.
(25) Androulakis, J.; Lee, Y.; Todorov, I.; Chung, D. Y.; Kanatzidis, M. *Phys. Rev. B* **2011**, *83*, 195209.
(26) Androulakis, J.; Chung, D. Y.; Su, X.; Zhang, L.; Uher, C.; Kanatzidis, M. G. *Phys. Rev. B* **2011**, *84*, 155207.
(27) Zhang, Q. Y.; Wang, H.; Liu, W. S.; Wang, H. Z.; Yu, B.; Zhang, Q.; Tian, Z. T.; Ni, G.; Lee, S.; Esfarjani, K.; Chen, G.; Ren, Z. F. *Energy Environ. Sci.* **2012**, *5*, 5246.
(28) Wang, S. Y.; Zheng, G.; Luo, T. T.; She, X. Y.; Li, H.; Tang, X. F. *J. Phys. D: Appl. Phys.* **2011**, *44*, 475304.
(29) Alekseeva, G. T.; Gurieva, E. A.; Konstantinov, P. P.; Prokof'eva, L. V.; Fedorov, M. I. *Semiconductors* **1996**, *30*, 1125.
(30) Nemov, S. A.; Gurieva, T. A.; Konstantinov, P. P.; Prokof'eva, L. V.; Proshin, M. I. *Semiconductors* **1998**, *32*, 689.
(31) Jovovic, V.; Thiagarajan, S. J.; West, J.; Heremans, J. P.; Story, T.; Golacki, Z.; Paszkowicz, W.; Osinniy, V. *J. Appl. Phys.* **2007**, *102*, 043707.
(32) Schlichting, U.; Gobrecht, K. H. *J. Phys. Chem. Solids* **1973**, *34*, 753.
(33) Kaĭdanov, V. I.; Mel'nik, R. B.; Germanas, N. V. *Sov. Phys. Semicond.* **1972**, *6*, 627.
(34) Prokof' eva, L. V.; Gurieva, E. A.; Zhumaksanov, Sh. M.; Konstantinov, P. P.; Maĭlina, Kh. R.; Ravich, Yu. I.; Stil'bans, L. S. *Sov. Phys. Semicond.* **1987**, *21*, 1078.
(35) Kaĭdanov, V. I.; Nemov, S. A.; Ravich, Yu. I. *Sov. Phys. Semicond.* **1992**, *26*, 113.
(36) Peng, H. W.; Song, J. H.; Kanatzidis, M. G.; Freeman, A. J. *Phys. Rev. B* **2011**, *84*, 125207.
(37) Heremans, J. P.; Wiendlocha, B.; Chamoire, A. M. *Energy Environ. Sci.* **2012**, *5*, 5510.
(38) Jaworski, C. M.; Wiendlocha, B.; Jovovic, V.; Heremans, J. P. *Energy Environ. Sci.* **2011**, *4*, 4155.
(39) Yan, X.; Poudel, B.; Ma, Y.; Liu, W. S.; Joshi, G.; Wang, H.; Lan, Y. C.; Wang, D. Z.; Chen, G.; Ren, Z. F. *Nano Lett.* **2010**, *10*, 3373.
(40) Ravich, Y. I.; Efimova, B. A.; Smirnov, I. A. *Semiconducting Lead Chalcogenides*; Plenum Press: New York, 1970.
(41) Poudel, B.; Hao, Q.; Ma, Y.; Lan, Y.; Minnich, A.; Yu, B.; Yan, X.; Wang, D.; Muto, A.; Vashaee, D.; Chen, X.; Liu, J.; Dresselhaus, M. S.; Chen, G.; Ren, Z. F. *Science* **2008**, *320*, 634.